Immune Netw. 2020 Oct;20(5):e40
https://doi.org/10.4110/in.2020.20.e40
pISSN 1598-2629·eISSN 2092-6685

IMMUNE NETWORK

Original Article

GRIM-19 Ameliorates Multiple Sclerosis in a Mouse Model of Experimental Autoimmune Encephalomyelitis with Reciprocal Regulation of IFNγ/Th1 and IL-17A/Th17 Cells

Jeonghyeon Moon [1,2,†], Seung Hoon Lee [3,†], Seon-yeong Lee [3,†], Jaeyoon Ryu [3], Jooyeon Jhun [3], JeongWon Choi [3], Gyoung Nyun Kim [4], Sangho Roh [2], Sung-Hwan Park [5], Mi-La Cho [1,3,6,*]

[1]Laboratory of Immune Network, Conversant Research Consortium in Immunologic Disease, College of Medicine, The Catholic University of Korea, Seoul 06591, Korea
[2]Cellular Reprogramming and Embryo Biotechnology Laboratory, Dental Research Institute, BK21 PLUS Dental Life Science, Seoul National University School of Dentistry, Seoul 08826, Korea
[3]Rheumatism Research Center, Catholic Research Institute of Medical Science, College of Medicine, The Catholic University of Korea, Seoul 06591, Korea
[4]College of Medicine, The Catholic University of Korea, Seoul 06591, Korea
[5]Division of Rheumatology, Department of Internal Medicine, Seoul St. Mary's Hospital, College of Medicine, The Catholic University of Korea, Seoul 06591, Korea
[6]Department of Medical Lifescience, College of Medicine, The Catholic University of Korea, Seoul 06591, Korea

Received: Jul 22, 2020
Revised: Sep 5, 2020
Accepted: Sep 23, 2020

***Correspondence to**
Mi-La Cho
Rheumatism Research Center, Catholic Institutes of Medical Science, College of Medicine, The Catholic University of Korea, 222 Banpo-daero, Seocho-gu, Seoul 06591, Korea.
E-mail: iammila@catholic.ac.kr

[†]Jeonghyeon Moon, Seung Hoon Lee, and Seon-yeong Lee contributed equally to this work.

ORCID iDs
Jeonghyeon Moon
https://orcid.org/0000-0002-5384-4077
Mi-La Cho
https://orcid.org/0000-0001-5715-3989

Conflicts of Interests
The authors declare no potential conflicts of interest.

ABSTRACT

The protein encoded by the Gene Associated with Retinoid-Interferon-Induced Mortality-19 (GRIM-19) is located in the mitochondrial inner membrane and is homologous to the NADH dehydrogenase 1-alpha subcomplex subunit 13 of the electron transport chain. Multiple sclerosis (MS) is a demyelinating disease that damages the brain and spinal cord. Although both the cause and mechanism of MS progression remain unclear, it is accepted that an immune disorder is involved. We explored whether GRIM-19 ameliorated MS by increasing the levels of inflammatory cytokines and immune cells; we used a mouse model of experimental autoimmune encephalomyelitis (EAE) to this end. Six-to-eight-week-old male C57BL/6, IFNγ-knockout (KO), and GRIM-19 transgenic mice were used; EAE was induced in all strains. A GRIM-19 overexpression vector (GRIM19 OVN) was electrophoretically injected intravenously. The levels of Th1 and Th17 cells were measured via flow cytometry, immunofluorescence, and immunohistochemical analysis. IL-17A and IFNγ expression levels were assessed via ELISA and quantitative PCR. IL-17A expression decreased and IFNγ expression increased in EAE mice that received injections of the GRIM19 OVN. GRIM-19 transgenic mice expressed more IFNγ than did wild-type mice; this inhibited EAE development. However, the effect of GRIM-19 overexpression on the EAE of IFNγ-KO mice did not differ from that of the empty vector. GRIM-19 expression was therapeutic for EAE mice, elevating the IFNγ level. GRIM-19 regulated the Th17/Treg cell balance.

Keywords: Gene Associated with Retinoid-Interferon-Induced Mortality-19; Multiple sclerosis; Experimental autoimmune encephalomyelitis; IL-17; IFNγ

IMMUNE NETWORK

Abbreviations

APC, allophycocyanin; CA, conus ammonis; CNS, central nervous system; DG, dentate gyrus; dLN, draining lymph node; EAE, experimental autoimmune encephalomyelitis; GRIM-19, Gene Associated with Retinoid-Interferon-Induced Mortality-19; GRIM19 OVN, GRIM-19 overexpression vector; GRIM19 TG, GRIM-19 transgenic; JC-1, 5,5′,6,6′-tetrachloro-1,1′,3,3′-tetraethylbenzimidazolcarbocyanine iodide; KO, knockout; MACS, magnetically activated cell sorting; MS, multiple sclerosis; NDUFA13, NADH dehydrogenase 1-alpha subcomplex subunit 13; PE, phycoerythrin; qPCR, quantitative PCR; SO, stratum oriens; SP, stratum pyramidale; SPF, specific pathogen-free; SR, stratum radiatum; TBST, Tris-buffered saline with 0.1% (v/v) Tween-20; WT, wild-type.

Author Contributions

Conceptualization: Moon J, Lee SH, Lee SY, Jhun J, Roh S, Cho ML; Data curation: Moon J, Lee SH, Choi J; Investigation: Moon J, Lee SY, Kim GN; Methodology: Ryu J, Choi J; Supervision: Park SH, Cho ML; Writing - original draft: Moon J.

INTRODUCTION

The Gene Associated with Retinoid-Interferon-Induced Mortality-19 (GRIM-19) encodes a nuclear protein homologous to the NADH dehydrogenase 1-alpha subcomplex subunit 13 (NDUFA13), and tends to induce apoptosis in interferon (IFN)- and all-*trans*-retinoic acid (RA)-induced tumor cells (1). GRIM-19 was showed that the inhibitor of tumor cells by activating IFN family and retinoic acid (2). GRIM-19 gene is located in chromosome 19 in genomic DNA in human, GRIM-19 binds to STAT3 directly in the cytosol and locates mitochondrial membrane (3,4). GRIM-19 is a protein of the mitochondrial inner membrane, being a component of the five electron transport chain complexes that produce cellular energy. GRIM-19 is closely involved in early embryonic development (5), controlling normal tissue development and suppressing tumor formation (6). GRIM-19 controls cell growth and death by targeting multiple proteins/pathways. Cell death is induced by GRIM-19 overexpression; cell growth is induced when GRIM-19 is suppressed (7). Not only is GRIM-19 associated with the development of tumors including osteosarcoma (8), hepatocellular carcinoma (9), lung cancer (10), cervical cancer (11), and prostate cancer (12) but the protein may also be associated with spontaneous abortion (13).

The etiology of multiple sclerosis (MS), an inflammatory, demyelinating, chronic neurodegenerative disorder of the central nervous system, remains elusive (14-17), but is widely thought to reflect abnormal T cell autoimmune destruction of oligodendrocytes and neurons (18). About 2.3 million people are affected globally; approximately 20,000 die annually (19). MS develops between the ages of 20 to 50 years and is more common in females (20). Although some drugs that slow the progression or alleviate the symptoms, no drugs have been developed to cure and the mechanism of disease onset is still unclear (21,22). The causes of MS include vitamin D deficiency, Epstein-Barr virus infection, intestinal bacterial flora, western diets and tobacco (23). To treat MS, use mesenchymal stem cells, anthracenedione antineoplastic agents, IL-1β inhibitors and α4-integrin humanized Abs (15,24,25). However, there is no clear cure method.

Of the several MS animal models, the autoimmune pathogenesis characteristic of MS is replicated in the model of experimental autoimmune encephalomyelitis (EAE) (26) characterized by the development of Abs targeting central nervous system (CNS) Ags such as the MBP-PLP fusion protein (MP4) and the Myelin Oligodendrocyte Glycoprotein ($MOG_{35–55}$ peptide) (27). EAE is an inflammatory demyelinating disease of the CNS (28) and serves as the prototype model of T cell-mediated autoimmune disease (29). We used the $MOG_{35–55}$ peptide to trigger EAE in C57BL/6 mice; this is a Th17 cell-dependent model (30). EAE models can be used to explore the mechanisms potentially involved in autoimmune conditions involving the CNS (31), including disease of the spine. Here, we used an EAE mouse model to determine the clinical significance of GRIM-19 expression and associated interferon production. Myelin-reactive T cells that produce IFNγ, IL-17, and GM-CSF are associated with the disabilities of EAE (32-37). Such disabilities are reduced by lowering the levels of pro-inflammatory cytokines including IFNγ and IL-17 (38-40). We induced EAE in GRIM-19 transgenic (GRIM19 TG) mice and IFNγ-knockout (KO) mice. We found a significant association between GRIM-19 and IFNγ status. We used GRIM-19 gene therapy to treat EAE mice; it may be possible to improve EAE employing such therapy.

MATERIALS AND METHODS

Animals

Six-to-eight-week-old male mice (strains C57BL/6 and IFNγ-KO) mice were purchased from Jackson Laboratory. Mouse GRIM-19 transgenic mice (C57BL/6 background) were purchased from Macrogen (Seoul, Korea). To establish this mouse line, a GRIM-19 fragment was inserted into the pcDNA3.1+ vector (Invitrogen, Waltham, MA, USA) containing the cytomegalovirus promoter by GenScript Corporation (Piscataway, NJ, USA) and microinjected by Macrogen. All animals were maintained under specific pathogen-free (SPF) conditions with free access to standard mouse chow (Ralston Purina, St. Louis, MO, USA) and water. The Animal Care Committee of The Catholic University of Korea approved the experimental protocol. All experimental procedures were evaluated and carried out in accordance with the protocols approved by the Animal Research Ethics Committee at the Catholic University of Korea (ID number: CUMC-2017-0304-02). All procedures performed followed the ethical guidelines on animal use.

EAE model

EAE was induced by subcutaneous injection of 500 ng $MOG_{35–55}$ peptide in incomplete Freund's adjuvant (Chondrex, Redmond, WA, USA) with 500 ng inactivated *Mycobacterium tuberculosis* (Difco, Franklin Lakes, NJ, USA) supplemented by intravenous injection of 200 ng pertussis toxin (Sigma, St. Louis, MO, USA) on days 0 and 2. The mice were observed and scored on a scale of 0–5 (with gradations at intervals of 0.5, thus allowing intermediate scores): 0, no clinical signs; 1, loss of tail tone; 2, wobbly gait; 3, hindlimb paralysis; 4, hindlimb and forelimb paralysis; and 5, death. Scoring of pathology was conducted by 2 proficient technicians by a blind test. Each group contained 5 mice and all experiments were repeated 3 or more times.

Injection of GRIM-19

To produce a mouse GRIM-19 overexpression vector (GRIM19 OVN), a mouse GRIM-19 fragment (RefSeq: NM_023312.3) was synthesized by TOP Gene Technologies (Quebec, Canada); the codons were optimized for expression in mammalian cells. The construct was subcloned between the *Bam*HI and *Xho*I sites of pcDNA3.1+. Mice were intravenously injected with 100 μg of this mouse GRIM19 OVN in 1 mL saline. The vector which was applied control groups was used empty mock vector. All vectors were injected per weekly, a total five injections. The vectors were delivered following hydrodynamic gene delivery (41). Then, mice were sacrificed and analyzed. The sequential experimental process were represented (**Fig. 1A**).

Immunohistochemistry

Spinal cord tissues were paraffin-embedded and 4-μm-thick sections stained with H&E. The spleens were fixed in 4% (v/v) paraformaldehyde, embedded in paraffin, and 4-μm-thick sections were deparaffinized in xylene and dehydrated in ascending baths of 70%–100% (v/v) ethanol. At least four sections from each tissue were analyzed. Immunohistochemistry employed the Vecta ABC kit (Vector Laboratories, Burlingame, CA, USA). Tissue sections were incubated with primary anti-IL-17A Ab overnight at 4°C, followed by a biotinylated secondary Ab and a streptavidin-peroxidase complex for 1 h. The final color was developed using 3,3-diaminobenzidine (Dako, Carpinteria, CA, USA) and the sections counterstained with Mayer's hematoxylin. Images were captured by a DP71 digital camera (Olympus, Center Valley, PA, USA) fitted to an Olympus BX41 microscope.

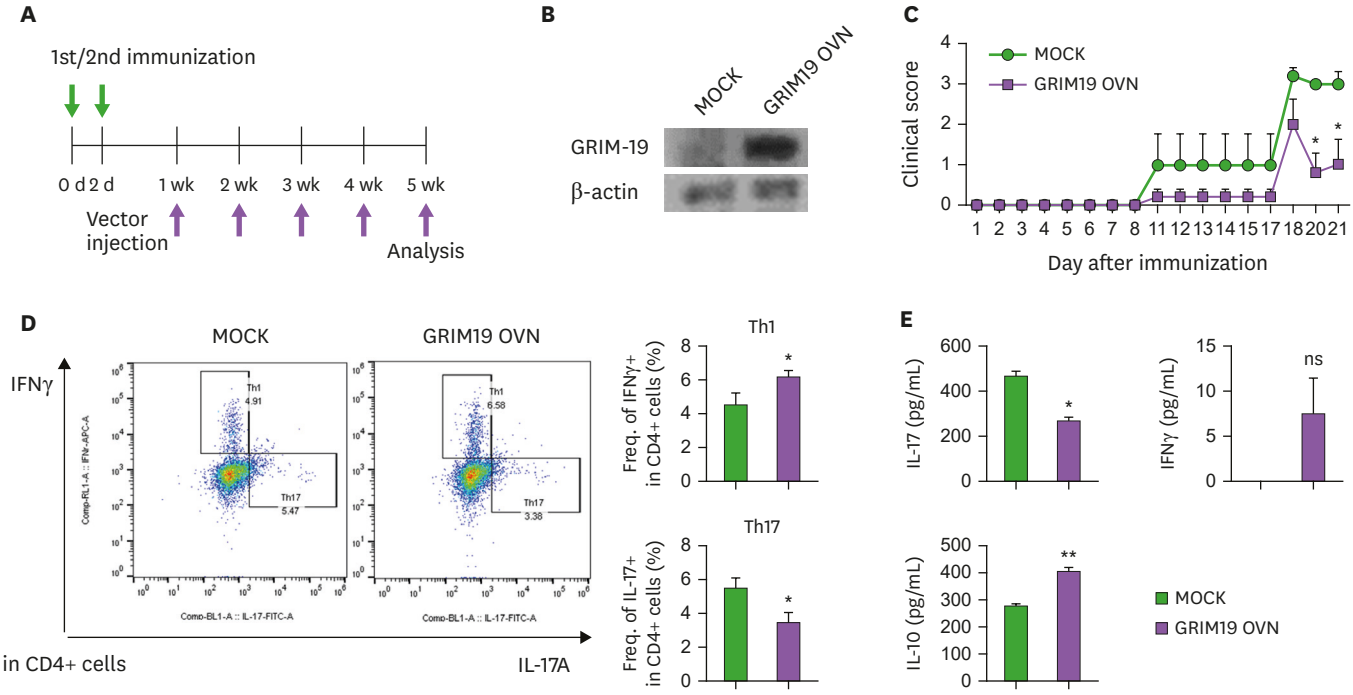

Figure 1. The IL-17A level decreased and that of IFNγ increased in mice with EAE that overexpressed GRIM-19 (n=5). (A) Schematic representation of the experiments. (B) Mock and GRIM19 OVN were assessed by western blotting. (C) The clinical scores of mock-injected and GRIM-19-injected mice. (D) After 5 wk, the mice were sacrificed and the splenocytes of the mice were isolated and analyzed. Th17 and Treg cell numbers in splenocyte populations were measured via *ex vivo* cell flow cytometry. (E) The IL-17A, IL-10, and IFNγ levels (as revealed by ELISA) in the culture media of mouse splenocytes cultured under conditions triggering Th17 differentiation (n=5).
*p<0.05, **p<0.01.

Immunostaining for confocal microscopy

Spleen cryosections (5-μm-thick) were stained with phycoerythrin (PE)-conjugated rat anti-mouse CD4 (45-0042-82; eBioscience, Waltham, MA, USA), PE-conjugated mouse anti-mouse GRIM-19 (sc-365978; Santa Cruz Biotechnology, Santa Cruz, TX, USA), FITC-conjugated rat anti-mouse IL-17A (11-7177-81; eBioscience), FITC-conjugated rat anti-mouse IFNγ (505810; BioLegend, San Diego, CA, USA), FITC-conjugated rat anti- mouse CD25 (102006; BioLegend), and rat allophycocyanin (APC)-conjugated mouse anti-Foxp3 (77-5775-40; eBioscience) Abs overnight at 4°C and the stained sections observed under a Zeiss confocal microscope (LSM 510 Meta; Carl Zeiss, Jena, Germany). Numbering of stained-cells was conducted by 2 proficient technicians by a blind test. Each group contained 5 mice and all experiments were repeated three times.

Western blotting

Lysates were centrifuged, proteins were loaded onto 10% (w/v) polyacrylamide gels, subjected to sodium dodecyl sulfate-polyacrylamide gel electrophoresis, and transferred to nitrocellulose membranes (Invitrogen). Membranes were blocked with 5% (w/v) skim milk in Tris-buffered saline with 0.1% (v/v) Tween-20 (TBST) for 1 h at room temperature. Abs against GRIM-19 and β-actin were added, followed by incubation at 4°C overnight. The membranes were reacted with goat anti-mouse HRP-conjugated Abs. Immunoreactivity was determined using an enhanced chemiluminescence system (Amersham Biosciences, Piscataway, NJ, USA).

https://doi.org/10.4110/in.2020.20.e40

Table 1. The PCR primers used

Gene	Sense (5′→3′)	Anti-sense (3′→5′)
β-actin	GAA ATC GTG CGT GAC ATC AAA G	TGT AGT TTC ATG GAT GCC ACA G
IL-17A	CCT CAA AGC TCA GCG TGT CC	GAG CTC ACT TTT GCG CCA AG
IFNγ	GAA AAT CCT GCA GAG CCA GA	TGA GCT CAT TGA ATG CTT GG

Quantitative PCR (qPCR) analysis

Total RNA was isolated with the TRIzol reagent (Molecular Research Center, Cincinnati, OH, USA). The concentrations of RNA were measured using a NanoDrop ND-1000 instrument (Thermo Fisher Scientific, Waltham, MA, USA). The 2-μg of RNA was reverse-transcribed into cDNA using a Transcriptor First-Strand cDNA Synthesis Kit (Roche Applied Science, Penzberg, Germany). The levels of mRNA were analyzed by qPCR employing a FastStart SYBR Green Master Mix (Roche Applied Science) and a StepOnePlus kit (Applied Biosystems, Foster City, CA, USA) following the manufacturers' instructions. The relative mRNA levels were normalized to those of β-actin. The primer sequences are listed in **Table 1**.

Measurement of 5,5′,6,6′-tetrachloro-1,1′,3,3′-tetraethylbenzimidazolcarbocyanine iodide (JC-1) by immunofluorescence

Splenocytes were isolated on 48-well plates and pretreated with 100 μm H2O2 for 2 h. After washing with PBS, the cells were stained with JC-1 (Invitrogen) solution for 30 min at 37°C and washed 3 times with PBS. The fluorescence intensity was detected by a CytoFluor multiwell plate reader at 514 nm for excitation and 529 nm for emission for green (monomer form) fluorescence, and 585 nm for excitation and 590 nm for emission for red (aggregate form) fluorescence.

Measurement of intracellular ROS and mitochondrial superoxide production

Mitochondrial superoxide levels were measured by mitoSOX RED staining according to the manufacturer's instructions. The splenocytes were treated with DOX and BAY60-2770, and then incubated with 2 μM of mitoSOX RED for 30 min at 37°C. After washing with PBS, red fluorescence was quantified with a fluorescence reader at excitation/emission wavelengths of 510/580 nm.

Flow cytometry

Cells that were for analysis of Th1 and Th17 population were stimulated with PMA and ionomycin with the GolgiSotp for 4 h (BD Biosciences, San Jose, CA, USA). To quantify Th1-, Th17-, and Foxp3-positive Treg cells, splenocytes were immunostained using a PerCp-conjugated anti-CD4 Ab (eBioscience) and fixed and permeabilized using a Cytofix/Cytoperm Plus kit (BD Biosciences). Following the manufacturer's instructions, splenocytes were stained with FITC-conjugated anti-IL-17A and APC-conjugated anti-IFNγ Abs (eBioscience). To identify Treg cells, splenocytes were surface-labeled with PerCp-conjugated anti-CD4 and APC-conjugated anti-CD25 Abs, followed by fixation, permeabilization, and intracellular staining with a PE-conjugated anti-Foxp3 Ab. All cells were detected using a FACS Calibur device (BD Pharmingen, Franklin Lakes, NJ, USA).

T-cell isolation, Th17 differentiation, and ELISAs

To determine the levels of IFNγ, IL-17A, and IL-10 expressed under conditions of Th17 differentiation, murine splenocytes were cultured in RPMI 1640 medium supplemented with 5% (v/v) FBS. CD4-positive T cells were sorted employing CD4-coated magnetic beads and a magnetically activated cell sorting (MACS) separation column (Miltenyi Biotec, Bergisch Gladbach, Germany). CD4-positive T cells were stimulated by addition of anti-CD3 (0.5 μg/mL)

and soluble anti-CD28 Abs (1 μg/mL; both from BD Biosciences), anti-IFNγ (2 μg/mL) and anti-IL-4 (2 μg/mL) Abs (Invitrogen), recombinant TGF-β (2 ng/mL), and recombinant IL-6 (20 ng/mL) (R&D Systems, Minneapolis, MN, USA) for 3 days. Culture supernatants were subjected to sandwich ELISAs (R&D Systems). Alkaline phosphatase (Sigma) was used for color development. Absorbance was determined at a wavelength of 405 nm using an ELISA microplate reader (Molecular Devices, San Jose, CA, USA).

Statistical analysis

All between-group comparisons were made using the nonparametric Mann-Whitney *U* test; all among-group (3 or more) comparisons were conducted via 1-way analysis of variance with Bonferroni's *post hoc* test. GraphPad Prism software (ver. 5.01) was employed for all analyses. A p-value <0.05 was considered statistically significant. Data are expressed as means±SDs.

RESULTS

The severity of EAE pathology was reduced by GRIM-19 overexpression via reduction of IL-17A levels

First, the pcDNA3.1+ hosting GRIM-19 (GRIM19 OVN) vector and mock vector were injected to EAE mice for 5 wk at 1-wk intervals (**Fig. 1A**). GRIM19 OVN vector and mock vector were transfected in HEK293 cells. Then, the lysates of cells were determined by western blotting for verifying of overexpression of GRIM-19 (**Fig. 1B**). To explore whether GRIM-19 overexpression reduced EAE pathology, we injected GRIM19 OVN into EAE mice. The clinical score was significantly lower in GRIM19 OVN- than mock vector-injected mice (**Fig. 1C**). Splenocytes were subjected to flow cytometry (**Fig. 1D**). The proportion of Th1 cells was significantly increased and that of Th17 cells markedly decreased in GRIM19 OVN-injected-mice. Under conditions of Th17 differentiation, the IL-17A level fell in GRIM19 OVN injected-mice and that of IL-10 increased. Although the IFNγ level increased somewhat in the former mice, the between-group difference was not significant (**Fig. 1E**). Thus, GRIM-19 overexpression ameliorated EAE pathology.

GRIM-19 overexpression was therapeutically efficacious

To investigate the lymphocyte transition, spleen cryosections were stained using anti-GRIM-19, -IL-17A, -CD25, and -Foxp3 Abs for immunofluorescence analyses. In GRIM19 OVN mice, GRIM-19 expression was significantly elevated in splenic lymphocytes and the Th17 population was significantly decreased. However, the Foxp3-positive Treg cell numbers did not differ significantly between mice injected with the empty vector and the GRIM19 OVN construct (**Fig. 2A**). Lymphocyte infiltration into the spinal cord of mock-injected mice was higher in the former than the latter mice (**Fig. 2B**). The paraffin sections revealed spinal cord damage. The spinal cord surface of empty vector-injected EAE mice was damaged by lymphocyte infiltration; the spinal cord of mice injected with the GRIM19 OVN construct was not. Immunohistochemical images revealed lower IL-17A expression in the spinal cord of GRIM19 OVN than empty vector-injected mice (**Fig. 2C**). The H&E staining data showed the hippocampal neurons in the mock injected mice and GRIM19 OVN injected mice (**Fig. 2D**). The neurons of in the GRIM19 OVN group exhibited clear cell layer compared to mock group. Thus, GRIM-19 overexpression reduced spinal cord and brain damage in EAE mice.

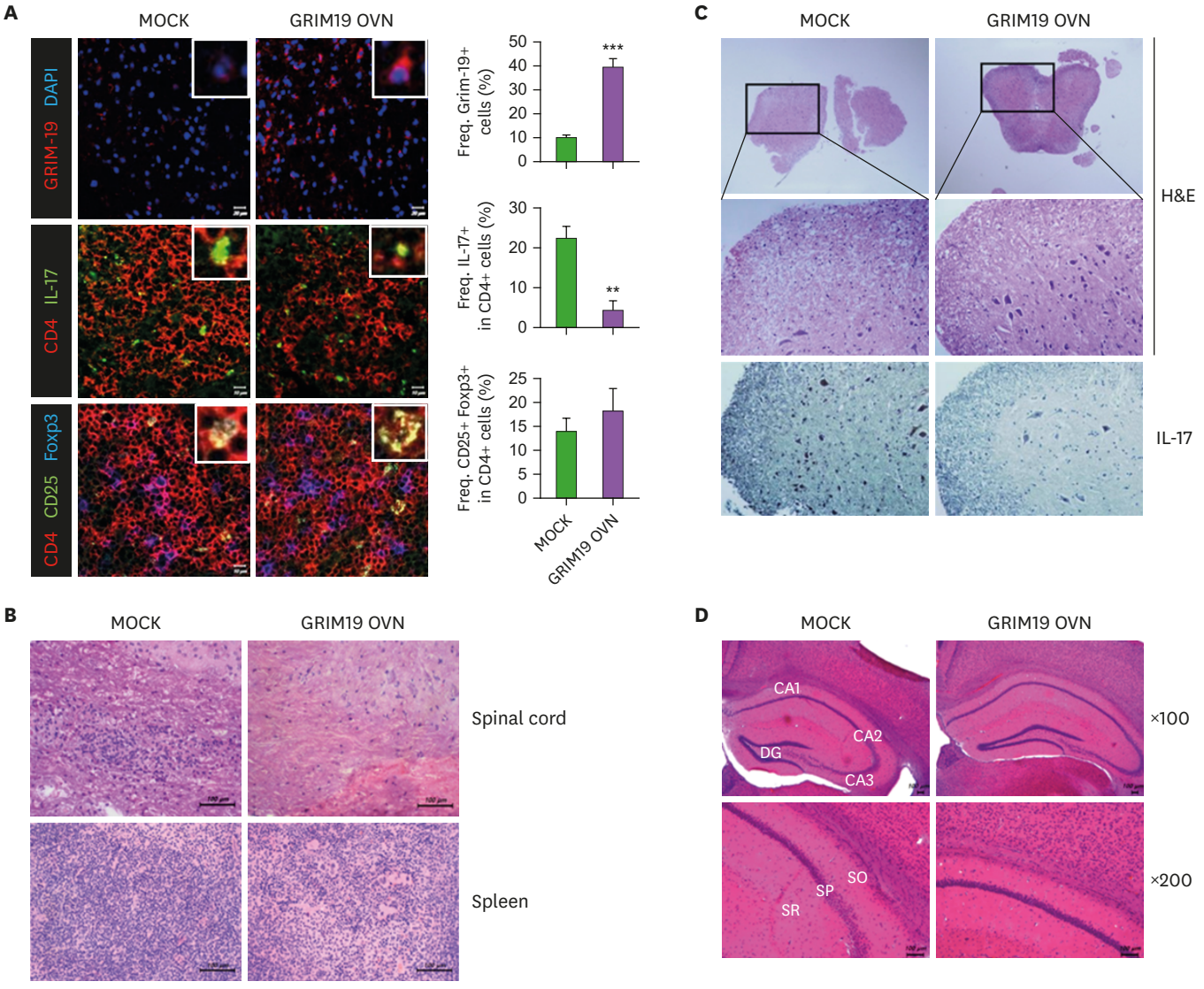

Figure 2. GRIM-19 overexpression was therapeutic in EAE mice. (A) After end of the experiment, immunofluorescent spleen images derived via confocal microscopy. GRIM-19+ cells (scale bars=20 μm), CD4+ IL-17A+ cells (scale bars=10 μm), and CD4+ CD25+ Foxp3+ cells (scale bars=10 μm) are evident (n=5). (B) After sacrifice of mice, Spinal cord and spleen sections stained with H&E (scale bars=100 μm). (C) Deparaffinized spinal cord sections stained with H&E (original magnifications ×50 and ×200, respectively), and immunohistochemically (original magnification, ×200). (D) The H&E images showed the hippocampal CA1-CA2 region.
**p<0.01, ***p<0.001.

EAE pathology was inhibited in GRIM TG mice via elevation of the IFNγ level and Treg cell numbers

We used GRIM19 TG mice to determine whether GRIM-19 overexpression inhibited the development of EAE symptoms. First, we established GRIM19 TG mice for experiments. GRIM-19 protein level was higher than WT mice in GRIM19 TG mice (**Fig. 3A**). The EAE clinical score of GRIM19 TG mice was significantly lower than that of the C57BL/6 EAE mice (**Fig. 3B**). The lymphocytes of the spleen and draining lymph nodes (dLNs) of each mouse were analyzed via flow cytometry. The populations of Treg cells were markedly higher in the spleen and dLNs of GRIM19 TG mice than control mice (**Fig. 3C**). In splenocytes, the Th1 cell population was significantly increased and Th17 level was reduced in GRIM19 TG mice (**Fig. 3D**). The serum levels of total IgG, IgG1, and IgG2a were significantly lower in GRIM19 TG mice than control C57BL/6 EAE mice (**Fig. 3E**). The population of IL-17 positive cells was

decreased in GRIM19 TG mice compared to WT (**Fig. 3F**). The H&E staining data showed the hippocampal neurons, the neurons of in the GRIM19 TG mice exhibited clear cell layer compared to WT mice (**Fig. 3G**). Thus, GRIM-19 inhibited EAE pathology by increasing the IFNγ level.

The mitochondrial function was improved in GRIM19 TG mice

To determine which difference has inhibition of EAE development in GRIM19 TG mice, we considered mitochondria change in GRIM19 TG mice to be different and investigated mitochondrial functions. Although there were no significant differences, the mitochondrial membrane potential was improved in GRIM19 TG mice through JC-1 staining (**Fig. 4A**). The population of mitochondria of splenocytes was increased in GRIM-19 TG mice (**Fig. 4B**). Besides, the mitochondrial superoxide was decreased in GRIM-19 TG mice significantly (**Fig. 4C**). The immunofluorescence images of transgenic mice showed a higher GRIM-19 expression of CD4-positive cells compared to WT mice (**Fig. 4D**). Therefore, this data suggested that the improvement of mitochondrial functions of GRIM19 TG mice may affect CD4-positive T cells.

EAE pathology was not inhibited in IFNγ-deficient mice injected with the GRIM-19 vector

To explore whether GRIM-19 overexpression reduced EAE pathology by elevating the IFNγ level, we established an IFNγ-KO mouse line. In such mice, neither the GRIM19 OVN construct nor the empty vector affected the clinical EAE score (**Fig. 5A**). The Th17 cell population was increased in the spleen of GRIM19 OVN injected IFNγ-KO mice, but the Treg cell population was not (**Fig. 5B**). Flow cytometry data of splenocytes showed that the population of Th1 and Th17 cells was slightly increased in GRIM19 OVN injected IFNγ-KO mice. However, there were no significant differences (**Fig. 5C**). The levels of mRNAs encoding IFNγ and IL-17A were measured via qPCR. The level of mRNA encoding IFNγ was markedly increased and that encoding IL-17A decreased in GRIM19 OVN injected WT mice. However, the mRNA expression of IFNγ and IL-17A of IFNγ-KO mice has no significant differences between mock and GRIM10 OVN injection groups (**Fig. 5D**). Thus, GRIM-19 overexpression did not affect EAE symptoms under IFNγ-deficient conditions.

DISCUSSION

We showed that GRIM-19 inhibited EAE progression. GRIM-19 overexpression reduced the Th17 population in EAE mice. Notably, GRIM-19 inhibited EAE development only in the presence of IFNγ. In previous studies, GRIM-19 increases interferon family as cell death regulatory protein through inhibition of STAT3 (1,4). GRIM-19 elevates the IFNβ and combination of retinoic acid, it regulates cell death related genes (42). GRIM-19 overexpression increased the IFNγ level to alleviate EAE pathology in EAE mice. GRIM-19 is a subunit of an NADH dehydrogenase that plays a critical role in the mitochondrial inner membrane (43). Although GRIM-19 was first used to inhibit cancer cell proliferation, recent studies found that GRIM-19 played roles in chronic inflammatory diseases including Crohn's disease and inflammatory bowel disease; GRIM-19 expression was reduced in such patients (44). GRIM-19 acts as an anti-bacterial regulator in the context of CARD15-mediated innate mucosal responses; GRIM-19 modulates the intestinal epithelial cell responses to microbial infection (45). However, it is unclear how GRIM-19 regulates inflammation. Thus, we explored the relevance of GRIM-19 in another inflammatory disease, EAE.

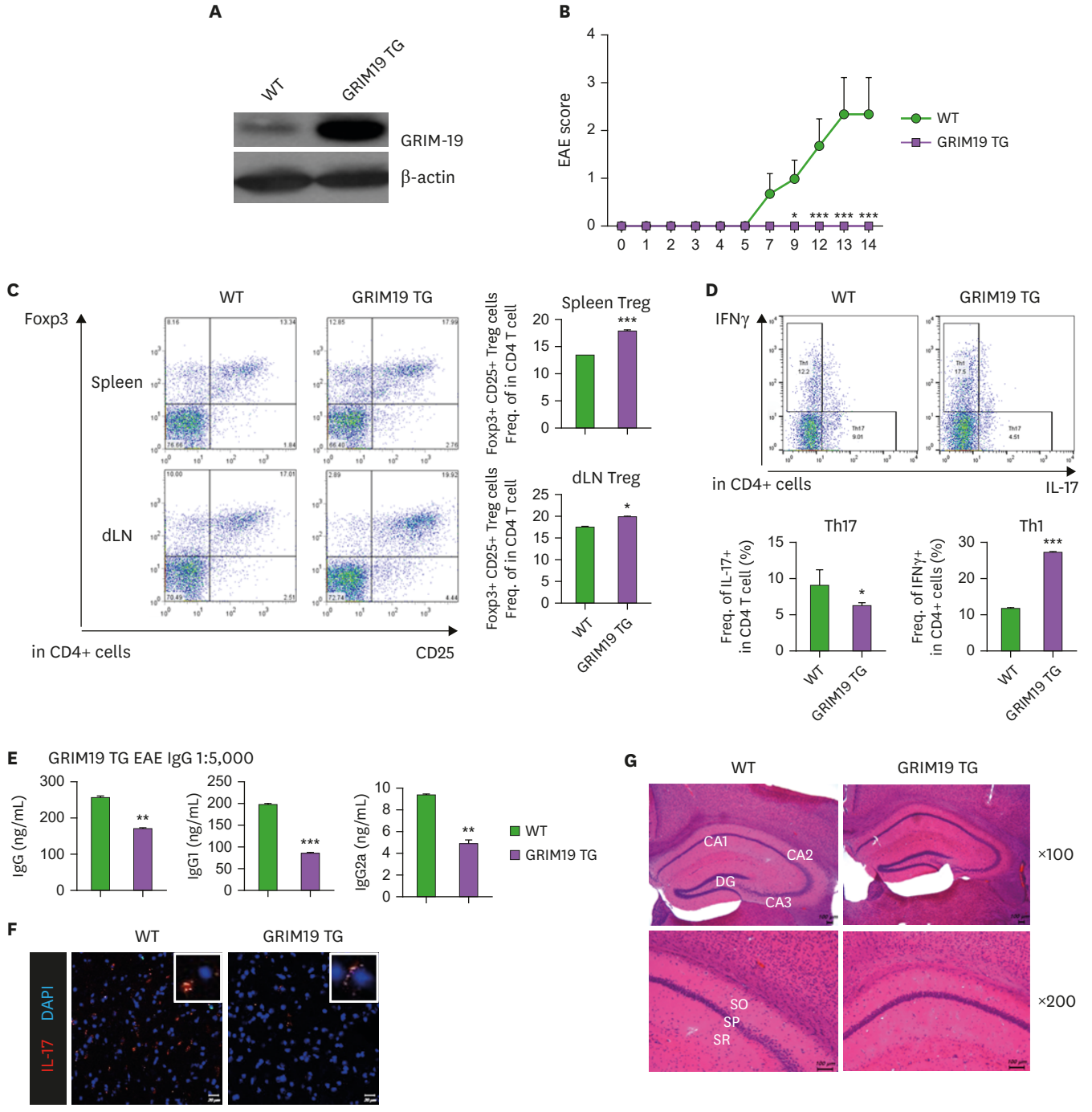

Figure 3. The development of EAE pathology was inhibited in GRIM19 TG mice. (A) GRIM-19 protein levels (assessed by Western blotting using anti-GRIM-19 and anti-β-actin Abs) in splenocyte lysates from WT and GRIM19 TG mice. (B) The clinical scores of WT EAE mice and GRIM19 TG mice. (C) After the end of the experiment, the splenocytes were isolated. Then, CD4+ CD25+ Foxp3+ Treg cell numbers were measured via flow cytometry in spleens and dLNs (n=5). (D) The IFNγ+ and IL-17A+ population of CD4+ splenocyte as measured via flow cytometry (n=5). (E) Before sacrificing the mice, the serum was collected. The concentrations of total IgG, IgG1, and IgG2a in serum were detected by ELISA (n=5). (F) The immunofluorescence images showed the IL-17 positive cell population of spleen tissues in WT and GRIM19 TG mice. (G) The H&E staining monitored the hippocampal region.
*p<0.05, **p<0.01, ***p<0.001.

We previously showed that GRIM-19 reduced progression of inflammatory bowel disease, graft-versus-host disease, and autoimmune arthritis, by regulating Th17 and Treg cell numbers (46-48). To explore whether GRIM-19 overexpression regulated the clinical pathology of EAE

https://doi.org/10.4110/in.2020.20.e40

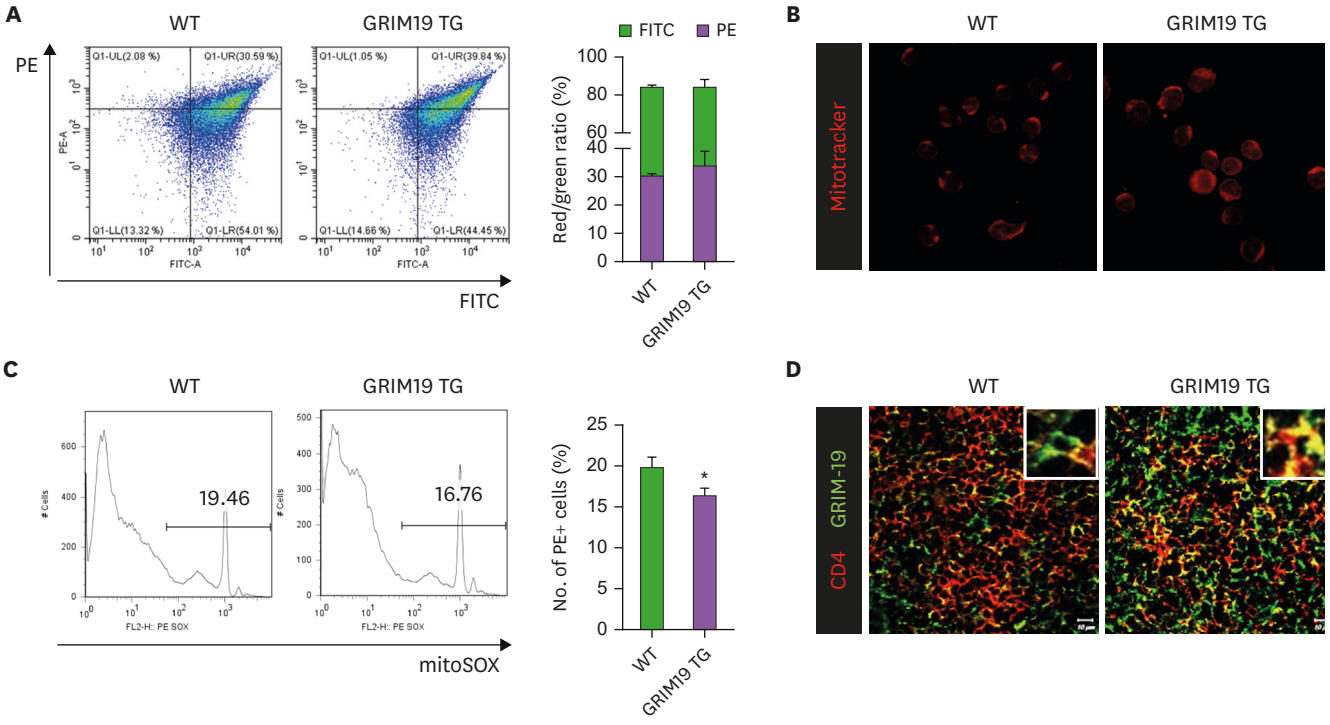

Figure 4. GRIM-19 overexpression induces the mitochondrial functions. (A) Mitochondrial membrane potential was detected using JC-1 dye for flow cytometry. (B) The confocal microscopy images showed the number of mitochondria in mice splenocytes. (C) The mitochondrial superoxide of splenocytes was measured by mitoSOX Red staining production assay. (D) The immunofluorescence images exhibited the CD4 and GRIM-19 double-positive cells.
*p<0.05.

mice, we injected a GRIM-19 overexpression construct (32) and the empty vector into EAE mice via intravenous electrophoresis. Notably, the IFNγ level increased and that of IL-17A decreased in such mice. These data were confirmed *in vitro* using splenocytes that were Th17-differentiated. Lymphocyte infiltration into the spinal cord was reduced in GRIM19 OVN-injected mice; GRIM-19 protected the spinal cord by inhibiting lymphocyte infiltration.

We used GRIM19 TG mice to explore whether GRIM-19 overexpression delayed EAE development. The EAE clinical score of such mice was much lower than that of control mice. In the former animals, the numbers of splenic IFNγ-expressing CD4-positive T cells increased. Although the IL-17A levels did not differ significantly between the groups, the level was somewhat lower in GRIM19 TG mice (**Fig. 3D**). Treg cell numbers increased in the spleen and dLNs of GRIM19 TG mice, and the serum IgG level decreased. Together, the data indicate that GRIM-19 overexpression regulated the immune response of EAE mice by modulating Th17 and Treg cell numbers. In both GRIM19 OVN-injected and GRIM19 TG mice, the IFNγ level was elevated.

We previously showed that an increased IFNγ level retarded the progression of rheumatoid arthritis (an autoimmune disease) by reducing Th17 cell numbers (49). Rheumatoid arthritis progression was more rapid in IFNγ-KO mice (50). IFNγ affects the innate and adaptive immune cells of EAE mice differently (51). The mechanism of IFNγ remains unclear. Although IFNγ has two-faced function in autoimmune diseases, induction of IFNγ has protective effect in EAE mouse (52) and decreases the level of IL-17A (51). IFNγ deficient mice which were IFNγ KO and anti-IFNγ Ab injected mice had severe EAE pathology and

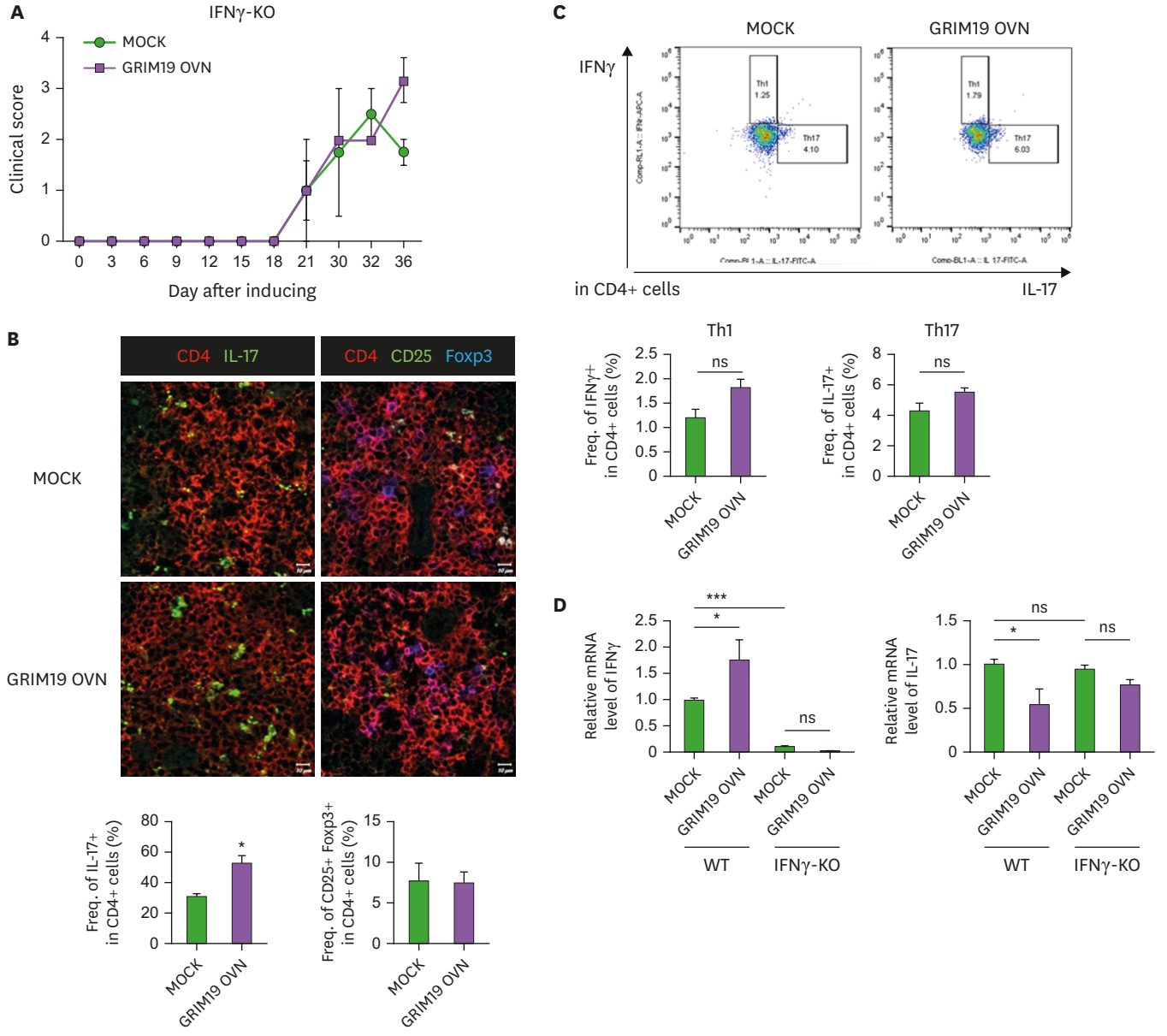

Figure 5. The pathology of EAE did not differ significantly in IFNγ-deficient mice given GRIM-19 gene therapy, compared to those that were not. (A) The clinical EAE scores of IFNγ-KO mice injected with the GRIM19 OVN construct and the empty vector. (B) After sacrifice of mice, immunofluorescent images of spleens stained with anti-CD4, anti-IL-17A, anti-CD25, and anti-Foxp3 Abs detecting Th17 and Foxp3+Treg cells (scale bars=10 μm) (n=5). (C) Th1 and Th17 cells which were isolated from splenocytes numbers measured via flow cytometry (n=5). (D) qPCR data showing the expression levels of IL-17A and IFNγ in splenocytes (n=5).
*p<0.05, **p<0.01, ***p<0.001.

an increase of immune cells in IFN gamma KO mice and anti-IFN-gamma injected mice (53). Especially, the treatment of IFNγ in EAE mice decreased clinical symptoms under the conditions that type I (IFNα and IFNβ) IFN exists (54).

Some studies found that GRIM-19 expression affected interferon levels (5,55). We hypothesized that GRIM-19 expression might correlate to that of IFNγ; we explored this possibility using IFNγ-KO mice. As expected, GRIM-19 overexpression exerted no therapeutic effect in IFNγ-KO EAE mice. Th1 cell numbers were reduced in the spleen tissue cells and splenocytes of IFNγ-KO mice, but the Th17 cell numbers increased. At the mRNA level, IFNγ

https://doi.org/10.4110/in.2020.20.e40

expression decreased and that of IL-17A increased in IFNγ-KO mice. We found that GRIM-19 inhibited the development of EAE in mice by regulating the levels of IFNγ and IL-17A and protecting the spinal cord against lymphocyte infiltration.

The GRIM-19 study focused primarily on inhibiting cancer cell growth (56,57). In particular, it is widely known to inhibit tumors through the increase of the IFN family (13,58). Our study suggested that GRIM-19 overexpression decreased the pathology of EAE symptoms through elevating of IFNγ levels. Overexpression of GRIM-19 reduced the level of IL-17A. Taken together, these results showed that the GRIM-19 expression has potentially therapeutic in autoimmune disease patients. However, we have not shown how GRIM-19 regulates IL-17A and IFNγ in detail mechanism. Further work is required.

ACKNOWLEDGEMENTS

This research was supported by a grant of the Korea Health Technology R&D Project through the Korea Health Industry Development Institute (KHIDI), funded by the Ministry of Health & Welfare, Republic of Korea (grant number HI20C1496) and a grant of the Korea Health Technology R&D Project through the Korea Health Industry Development Institute (KHIDI), funded by the Ministry of Health & Welfare, Republic of Korea (grant number: HI15C3062).

REFERENCES

1. Huang G, Lu H, Hao A, Ng DC, Ponniah S, Guo K, Lufei C, Zeng Q, Cao X. GRIM-19, a cell death regulatory protein, is essential for assembly and function of mitochondrial complex I. *Mol Cell Biol* 2004;24:8447-8456.
PUBMED | CROSSREF
2. Tian B, Zhao Y, Liang T, Ye X, Li Z, Yan D, Fu Q, Li Y. Curcumin inhibits urothelial tumor development by suppressing IGF2 and IGF2-mediated PI3K/AKT/mTOR signaling pathway. *J Drug Target* 2017;25:626-636.
PUBMED | CROSSREF
3. Lufei C, Ma J, Huang G, Zhang T, Novotny-Diermayr V, Ong CT, Cao X. GRIM-19, a death-regulatory gene product, suppresses Stat3 activity via functional interaction. *EMBO J* 2003;22:1325-1335.
PUBMED | CROSSREF
4. Zhang J, Yang J, Roy SK, Tininini S, Hu J, Bromberg JF, Poli V, Stark GR, Kalvakolanu DV. The cell death regulator GRIM-19 is an inhibitor of signal transducer and activator of transcription 3. *Proc Natl Acad Sci U S A* 2003;100:9342-9347.
PUBMED | CROSSREF
5. Kalvakolanu DV, Nallar SC, Kalakonda S. Cytokine-induced tumor suppressors: a GRIM story. *Cytokine* 2010;52:128-142.
PUBMED | CROSSREF
6. Kong D, Zhao L, Du Y, He P, Zou Y, Yang L, Sun L, Wang H, Xu D, Meng X, et al. Overexpression of GRIM-19, a mitochondrial respiratory chain complex I protein, suppresses hepatocellular carcinoma growth. *Int J Clin Exp Pathol* 2014;7:7497-7507.
PUBMED
7. Nallar SC, Kalakonda S, Sun P, Kalvakolanu DV. Grim-19: A double-edged sword that regulates anti-tumor and innate immune responses. *Transl Oncogenomics* 2008.3:67-79.
PUBMED
8. Chen W, Liu Q, Fu B, Liu K, Jiang W. Overexpression of GRIM-19 accelerates radiation-induced osteosarcoma cells apoptosis by p53 stabilization. *Life Sci* 2018;208:232-238.
PUBMED | CROSSREF
9. Li F, Ren W, Zhao Y, Fu Z, Ji Y, Zhu Y, Qin C. Downregulation of GRIM-19 is associated with hyperactivation of p-STAT3 in hepatocellular carcinoma. *Med Oncol* 2012;29:3046-3054.
PUBMED | CROSSREF

10. Wang T, Yan XB, Zhao JJ, Ye J, Jiang ZF, Wu DR, Xiao WH, Liu RY. Gene associated with retinoid-interferon-induced mortality-19 suppresses growth of lung adenocarcinoma tumor *in vitro* and *in vivo*. *Lung Cancer* 2011;72:287-293.
PUBMED | CROSSREF
11. Zhou Y, Wei Y, Zhu J, Wang Q, Bao L, Ma Y, Chen Y, Feng D, Zhang A, Sun J, et al. GRIM-19 disrupts E6/E6AP complex to rescue p53 and induce apoptosis in cervical cancers. *PLoS One* 2011;6:e22065.
PUBMED | CROSSREF
12. Lin H, Shen Z, Liu H, Yang M, Lin J, Luo L, Liu L, Chen H. Upregulation of GRIM-19 augments the sensitivity of prostate cancer cells to docetaxel by targeting Rad23b. *Clin Exp Pharmacol Physiol* 2020;47:76-84.
PUBMED | CROSSREF
13. Chen H, Deng X, Yang Y, Shen Y, Chao L, Wen Y, Sun Y. Expression of GRIM-19 in missed abortion and possible pathogenesis. *Fertil Steril* 2015;103:138-46.e3.
PUBMED | CROSSREF
14. Fjær S, Bø L, Myhr KM, Torkildsen Ø, Wergeland S. Magnetization transfer ratio does not correlate to myelin content in the brain in the MOG-EAE mouse model. *Neurochem Int* 2015;83-84:28-40.
PUBMED | CROSSREF
15. Galea I, Ward-Abel N, Heesen C. Relapse in multiple sclerosis. *BMJ* 2015;350:h1765.
PUBMED | CROSSREF
16. Lorscheider J, Buzzard K, Jokubaitis V, Spelman T, Havrdova E, Horakova D, Trojano M, Izquierdo G, Girard M, Duquette P, et al. Defining secondary progressive multiple sclerosis. *Brain* 2016;139:2395-2405.
PUBMED | CROSSREF
17. Owens B. Multiple sclerosis. *Nature* 2016;540:S1.
PUBMED | CROSSREF
18. Bittner S, Afzali AM, Wiendl H, Meuth SG. Myelin oligodendrocyte glycoprotein (MOG35-55) induced experimental autoimmune encephalomyelitis (EAE) in C57BL/6 mice. *J Vis Exp* 2014:51275.
PUBMED | CROSSREF
19. Alharbi FM. Update in vitamin D and multiple sclerosis. *Neurosciences* 2015;20:329-335.
PUBMED | CROSSREF
20. Rolak LA. Multiple sclerosis: it's not the disease you thought it was. *Clin Med Res* 2003;1:57-60.
PUBMED | CROSSREF
21. Faguy K. Multiple sclerosis: an update. *Radiol Technol* 2016;87:529-550.
PUBMED
22. Garg N, Smith TW. An update on immunopathogenesis, diagnosis, and treatment of multiple sclerosis. *Brain Behav* 2015;5:e00362.
PUBMED | CROSSREF
23. Yadav SK, Mindur JE, Ito K, Dhib-Jalbut S. Advances in the immunopathogenesis of multiple sclerosis. *Curr Opin Neurol* 2015;28:206-219.
PUBMED | CROSSREF
24. Darlington PJ, Boivin MN, Renoux C, François M, Galipeau J, Freedman MS, Atkins HL, Cohen JA, Solchaga L, Bar-Or A. Reciprocal Th1 and Th17 regulation by mesenchymal stem cells: implication for multiple sclerosis. *Ann Neurol* 2010;68:540-545.
PUBMED | CROSSREF
25. Quiñones-Aguilar S, Sauri-Suárez S, Alcaraz-Estrada SL, García S. Progressive multifocal leukoencephalopathy associated to treatment with natalizumab in Mexican patient multiple sclerosis. Case report, analysis and update. *Neuroendocrinol Lett* 2019;40:222-226.
PUBMED
26. Procaccini C, De Rosa V, Pucino V, Formisano L, Matarese G. Animal models of multiple sclerosis. *Eur J Pharmacol* 2015;759:182-191.
PUBMED | CROSSREF
27. Kuerten S, Javeri S, Tary-Lehmann M, Lehmann PV, Angelov DN. Fundamental differences in the dynamics of CNS lesion development and composition in MP4- and MOG peptide 35-55-induced experimental autoimmune encephalomyelitis. *Clin Immunol* 2008;129:256-267.
PUBMED | CROSSREF
28. Linker RA, Lee DH. Models of autoimmune demyelination in the central nervous system: on the way to translational medicine. *Exp Transl Stroke Med* 2009;1:5.
PUBMED | CROSSREF
29. Bowles AC, Scruggs BA, Bunnell BA. Mesenchymal stem cell-based therapy in a mouse model of experimental autoimmune encephalomyelitis (EAE). *Methods Mol Biol* 2014;1213:303-319.
PUBMED | CROSSREF

30. Aranami T, Yamamura T. Th17 Cells and autoimmune encephalomyelitis (EAE/MS). *Allergol Int* 2008;57:115-120.
PUBMED | CROSSREF

31. Baker D, Amor S. Mouse models of multiple sclerosis: lost in translation? *Curr Pharm Des* 2015;21:2440-2452.
PUBMED | CROSSREF

32. Pettinelli CB, McFarlin DE. Adoptive transfer of experimental allergic encephalomyelitis in SJL/J mice after *in vitro* activation of lymph node cells by myelin basic protein: requirement for Lyt 1+ 2− T lymphocytes. *J Immunol* 1981;127:1420-1423.
PUBMED

33. Ando DG, Clayton J, Kono D, Urban JL, Sercarz EE. Encephalitogenic T cells in the B10.PL model of experimental allergic encephalomyelitis (EAE) are of the Th-1 lymphokine subtype. *Cell Immunol* 1989;124:132-143.
PUBMED | CROSSREF

34. Hofstetter HH, Ibrahim SM, Koczan D, Kruse N, Weishaupt A, Toyka KV, Gold R. Therapeutic efficacy of IL-17 neutralization in murine experimental autoimmune encephalomyelitis. *Cell Immunol* 2005;237:123-130.
PUBMED | CROSSREF

35. Ponomarev ED, Shriver LP, Maresz K, Pedras-Vasconcelos J, Verthelyi D, Dittel BN. GM-CSF production by autoreactive T cells is required for the activation of microglial cells and the onset of experimental autoimmune encephalomyelitis. *J Immunol* 2007;178:39-48.
PUBMED | CROSSREF

36. El-Behi M, Ciric B, Dai H, Yan Y, Cullimore M, Safavi F, Zhang GX, Dittel BN, Rostami A. The encephalitogenicity of T_H17 cells is dependent on IL-1- and IL-23-induced production of the cytokine GM-CSF. *Nat Immunol* 2011;12:568-575.
PUBMED | CROSSREF

37. Cummings M, Arumanayagam AC, Zhao P, Kannanganat S, Stuve O, Karandikar NJ, Eagar TN. Presenilin1 regulates Th1 and Th17 effector responses but is not required for experimental autoimmune encephalomyelitis. *PLoS One* 2018;13:e0200752.
PUBMED | CROSSREF

38. Giacoppo S, Pollastro F, Grassi G, Bramanti P, Mazzon E. Target regulation of PI3K/Akt/mTOR pathway by cannabidiol in treatment of experimental multiple sclerosis. *Fitoterapia* 2017;116:77-84.
PUBMED | CROSSREF

39. Hamana A, Takahashi Y, Tanioka A, Nishikawa M, Takakura Y. Amelioration of experimental autoimmune encephalomyelitis in mice by interferon-beta gene therapy, using a long-term expression plasmid vector. *Mol Pharm* 2017;14:1212-1217.
PUBMED | CROSSREF

40. Hou H, Miao J, Cao R, Han M, Sun Y, Liu X, Guo L. Rapamycin ameliorates experimental autoimmune encephalomyelitis by suppressing the mTOR-STAT3 pathway. *Neurochem Res* 2017;42:2831-2840.
PUBMED | CROSSREF

41. Suda T, Liu D. Hydrodynamic gene delivery: its principles and applications. *Mol Ther* 2007;15:2063-2069.
PUBMED | CROSSREF

42. Angell JE, Lindner DJ, Shapiro PS, Hofmann ER, Kalvakolanu DV. Identification of GRIM-19, a novel cell death-regulatory gene induced by the interferon-β and retinoic acid combination, using a genetic approach. *J Biol Chem* 2000;275:33416-33426.
PUBMED | CROSSREF

43. Lu H, Cao X. GRIM-19 is essential for maintenance of mitochondrial membrane potential. *Mol Biol Cell* 2008;19:1893-1902.
PUBMED | CROSSREF

44. Yamamoto-Furusho JK, Barnich N, Hisamatsu T, Podolsky DK. MDP-NOD2 stimulation induces HNP-1 secretion, which contributes to NOD2 antibacterial function. *Inflamm Bowel Dis* 2010;16:736-742.
PUBMED | CROSSREF

45. Strober W, Murray PJ, Kitani A, Watanabe T. Signalling pathways and molecular interactions of NOD1 and NOD2. *Nat Rev Immunol* 2006;6:9-20.
PUBMED | CROSSREF

46. Moon YM, Lee J, Lee SY, Her YM, Ryu JG, Kim EK, Son HJ, Kwok SK, Ju JH, Yang CW, et al. Gene associated with retinoid-interferon-induced mortality 19 attenuates murine autoimmune arthritis by regulation of Th17 and Treg cells. *Arthritis Rheumatol* 2014;66:569-578.
PUBMED | CROSSREF

47. Kim JK, Lee SH, Lee SY, Kim EK, Kwon JE, Seo HB, Lee HH, Lee BI, Park SH, Cho ML. Grim19 attenuates DSS induced colitis in an animal model. *PLoS One* 2016;11:e0155853.
PUBMED | CROSSREF

48. Park MJ, Lee SH, Lee SH, Kim EK, Lee EJ, Moon YM, La Cho M. GRIM19 ameliorates acute graft-versus-host disease (GVHD) by modulating Th17 and Treg cell balance through down-regulation of STAT3 and NF-AT activation. *J Transl Med* 2016;14:206.
PUBMED | CROSSREF

49. Lee J, Lee J, Park MK, Lim MA, Park EM, Kim EK, Yang EJ, Lee SY, Jhun JY, Park SH, et al. Interferon gamma suppresses collagen-induced arthritis by regulation of Th17 through the induction of indoleamine-2,3-deoxygenase. *PLoS One* 2013;8:e60900.
PUBMED | CROSSREF

50. Lee SH, Kwon JY, Kim SY, Jung K, Cho ML. Interferon-gamma regulates inflammatory cell death by targeting necroptosis in experimental autoimmune arthritis. *Sci Rep* 2017;7:10133.
PUBMED | CROSSREF

51. Arellano G, Ottum PA, Reyes LI, Burgos PI, Naves R. Stage-specific role of interferon-gamma in experimental autoimmune encephalomyelitis and multiple sclerosis. *Front Immunol* 2015;6:492.
PUBMED | CROSSREF

52. Miller NM, Wang J, Tan Y, Dittel BN. Anti-inflammatory mechanisms of IFN-γ studied in experimental autoimmune encephalomyelitis reveal neutrophils as a potential target in multiple sclerosis. *Front Neurosci* 2015;9:287.
PUBMED | CROSSREF

53. Sosa RA, Murphey C, Robinson RR, Forsthuber TG. IFN-γ ameliorates autoimmune encephalomyelitis by limiting myelin lipid peroxidation. *Proc Natl Acad Sci U S A* 2015;112:E5038-E5047.
PUBMED | CROSSREF

54. Naves R, Singh SP, Cashman KS, Rowse AL, Axtell RC, Steinman L, Mountz JD, Steele C, De Sarno P, Raman C. The interdependent, overlapping, and differential roles of type I and II IFNs in the pathogenesis of experimental autoimmune encephalomyelitis. *J Immunol* 2013;191:2967-2977.
PUBMED | CROSSREF

55. Kalakonda S, Nallar SC, Jaber S, Keay SK, Rorke E, Munivenkatappa R, Lindner DJ, Fiskum GM, Kalvakolanu DV. Monoallelic loss of tumor suppressor GRIM-19 promotes tumorigenesis in mice. *Proc Natl Acad Sci U S A* 2013;110:E4213-E4222.
PUBMED | CROSSREF

56. Kalakonda S, Nallar SC, Gong P, Lindner DJ, Goldblum SE, Reddy SP, Kalvakolanu DV. Tumor suppressive protein gene associated with retinoid-interferon-induced mortality (GRIM)-19 inhibits src-induced oncogenic transformation at multiple levels. *Am J Pathol* 2007;171:1352-1368.
PUBMED | CROSSREF

57. Nallar SC, Kalvakolanu DV. GRIM-19: a master regulator of cytokine induced tumor suppression, metastasis and energy metabolism. *Cytokine Growth Factor Rev* 2017;33:1-18.
PUBMED | CROSSREF

58. Song J, Shi W, Wang W, Zhang Y, Zheng S. Grim-19 expressed by recombinant adenovirus for esophageal neoplasm target therapy. *Mol Med Rep* 2018;17:6667-6674.
PUBMED | CROSSREF